Acta Univ. Sapientiae Informatica **15,** 1 (2023) 146–169

DOI: 10.2478/ausi-2023-0011

Enhanced imagistic methodologies augmenting radiological image processing in interstitial lung diseases

József PALATKA
Doctoral School of Applied Informatics and Applied Mathematics
University Research, Innovation and Service Center
Óbuda University, Budapest, Hungary
email: jozsef.palatka@syneoshealth.com

Levente KOVÁCS
University Research, Innovation and Service Center
Óbuda University, Budapest, Hungary
email: kovacs@uni-obuda.hu ORCID: 0000-0002-3188-0800

László SZILÁGYI
Computational Intelligence Research Group,
Sapientia Hungarian University of Transylvania,
Târgu Mureș, Romania
University Research, Innovation and Service Center
Óbuda University, Budapest, Hungary
Department of Mechanical Engineering
University of Canterbury,
Christchurch, New Zealand
email: lalo@ms.sapientia.ro
szilagyi.laszlo@uni-obuda.hu ORCID: 0000-0001-6722-2642

Key words and phrases: interstitial lung diseases, high-resolution computed tomography, radiography image processing, complex networks, convolutional neural networks, computer-aided diagnostics, deep learning, machine learning

Abstract. Interstitial Lung Diseases (ILDs) represent a heterogeneous group of several rare diseases that are difficult to predict, diagnose and monitor. There are no predictive biomarkers for ILDs, clinical signs are similar to the ones for other lung diseases, the radiological features are not easy to recognize, and require manual radiologist review. Data-driven support for ILD prediction, diagnosis and disease-course monitoring are great unmet need. Numerous image processing techniques and computer-aided diagnostic and decision-making support methods have been developed over the recent years. The current review focuses on such solutions, discussing advancements on the fields of Quantitative CT, Complex Networks, and Convolutional Neural Networks.

1 Introduction

Interstitial lung diseases (ILDs) refer to a group of over 200 diverse disorders that involve inflammation and progressive fibrosis of lung interstitium, representing an important morbidity and mortality cause. The incidence of ILD ranges from 1 to 31.5 per 100,000 person-years and prevalence ranged from 6.3 to 71 per 100,000 people [20]. It is more common in the elderly population, median age at diagnosis is over 60 years [26].

ILD causes inflammation and scarring (fibrosis) of the interstitium, making the oxygen difficult to pass into the bloodstream. This can result in symptoms such as shortness of breath, cough, fatigue, and chest pain. ILD can also cause a decreased tolerance for physical activity, and in more advanced cases, can lead to respiratory failure; besides being seriously debilitating, it is significantly affecting the patients' quality of life.

There are many different types of ILD, with overlapping clinical, radiological, and pathological features. The most common type is idiopathic pulmonary fibrosis (IPF), which is of unknown cause. Other ones that are more prevalent are: connective tissue disease-associated ILD in people with autoimmune diseases (e.g. rheumatoid arthritis and scleroderma), hypersensitivity pneumonitis, sarcoidosis, and drug-induced ILD (DIILD).

ILD is known to be difficult to diagnose and treat, and management typically involves a multidisciplinary approach made of medications, oxygen therapy, pulmonary rehabilitation, and lung transplantation. Treatment efficacy is usually measured by changes in pulmonary function (forced vital capacity – FVC), more precisely the reduction of FVC decline over time, changes of exercise tolerance, or progression-free survival.

Beyond the individual patient burden, the economic impact of ILD is also significant, both on a personal and societal level. Here are some factors that contribute to the economic burden of ILD.

1. Healthcare costs: ILD often requires a suite of highly specific diagnostic tools, including radiographic imaging, lung function tests, bronchoscopy, and sometimes lung biopsy. For the progressive nature of the disease, ongoing monitoring, medication management, and specialist oversight is necessary. The costs associated with these medical services, including hospitalizations, medications, and regular follow-up visits, contribute to the economic burden. The home care for these patients is also substantial (assistance with daily activities, transportation to medical appointments, and emotional support).

2. Treatment expenses: ILD treatment may involve a combination of medications, such as corticosteroids, immunosuppressants, and antifibrotic drugs, depending on the specific type of ILD. These medications can be costly, and the duration of treatment may extend over a long period, further increasing the financial impact. In severe cases of ILD, where conservative treatment options have been exhausted, lung transplantation remains the only option. Lung transplantation is a complex and expensive procedure with substantial associated costs.

3. Lost productivity: ILD can significantly impact a person's ability to work and engage in daily activities. Consequently, individuals with ILD may experience decreased work hours, reduced productivity, or even complete disability, leading to income loss and further diminished quality of life.

The drug-induced interstitial lung disease is a specific type of ILDs that deserves a separate evaluation. This is a heterogenous group of pulmonary parenchymal diseases that occur in relation to exposure to certain drugs. To-date 1,653 drugs and procedures are associated with ILDs, and the list is increasing. Medicines used in several disease areas are on the list including many highly promising oncology products that are meant to cover areas of great unmet need [11]. DIILDs are an outcome of a medication administered to patients, hence keeping it at lowest possible incidence is a moral obligation for the physicians and drug-makers. Furthermore, DIILDs are darkening the results of certain drugs that are otherwise highly successful (e.g. trastuzumab deruxtecan (T-DXd), Enhertu®, the most successful oncology product discovered in the recent years [25]) and are seriously limiting their use and their therapeutic potential.

2 Predicting, diagnosing and monitoring ILDs

Despite the recent advancements of technology and medicinal science, the effective management of patients with ILDs is still insufficient at three main levels: the early detection of ILD, accurate prognostication using baseline data, and accurate and precise monitoring of disease response to therapy through high-resolution computer tomography (HRCT) [6].

The diagnosis of ILDs is based on integrated clinical evaluation, pulmonary function tests, radiological assessments, lab tests and, in some cases, histopathological examination that involves the collaboration of a large multidisciplinary team.

ILDs should be considered in the differential diagnosis of adults presenting with unexplained exertional shortness of breath, chronic cough, and/or crackles on chest auscultation, especially when the common pulmonary disorders can be ruled out. ILDs classically produce the "3Cs": cough, clubbing of the nails, and coarse crackles on auscultation [32]. At clinical evaluation a detailed medical history is obtained, including environmental and drug exposure history, full body examination with focus on clinical signs on the patients' hand, joint, and skin. A review of the patients' medication is needed in search of agents that are known to cause DIILDs. Common drugs associated with ILD are cancer therapies (i.e., bleomycin, immune checkpoint inhibitors), rheumatologic agents, amiodarone, and antibiotics (i.e., nitrofurantoin) and several others. A thorough family history focusing on idiopathic interstitial pneumonia and autoimmune disease should also be performed.

Pulmonary function tests (PFTs) are done to assess lung function and help determine the presence and severity of restrictive or obstructive lung disease. They typically include measurements of lung volumes, and of the maximum amount of air a person can forcefully exhale after taking a deep breath (forced vital capacity – FVC); as well as diffusing capacity for carbon monoxide (DLCO), and spirometry. Patients with ILDs typically exhibit reduced FVC, reduced total lung volume, and reduced diffusing capacities, though these values may appear normal early in the disease course, and when combined pulmonary fibrosis and emphysema is present [8].

High-resolution computed tomography (HRCT) is a key imaging modality for evaluating ILDs. HRCT scans provide detailed images of lung structures, allowing the detection of characteristic patterns associated with different ILD subtypes. Radiological features, such as ground-glass opacities, reticular or honeycomb patterns, nodules, and distribution patterns, help guide the diagnosis and classification of ILDs. Computer-aided evaluation of HRCT images,

in support of ILD diagnosis is a rapidly developing area, but the breakthrough has not yet been achieved [30].

Serological and immunological blood tests may be conducted to assess markers, autoantibodies, or immunological abnormalities that could indicate an underlying connective tissue disease associated with ILDs, such as rheumatoid arthritis, systemic sclerosis, or sarcoidosis.

Cytological, or histopathological examination may be required to establish a definitive diagnosis and determine the underlying histopathological features. Bronchoalveolar lavage material or lung tissue obtained through biopsy helps identify the characteristics of the interstitial inflammation, fibrosis, or other specific changes, aiding in the classification of ILDs. Recently whole transcriptome RNA sequencing of the biopsy tissue sample was found successful in classifying ILDs. Gene expression analyses can help to distinguish between types of ILDs. These are areas of intensive ongoing research [26].

2.1 Clinical challenges

The prevalence of ILDs is low, and this already makes it difficult to be recognized. Their clinical features (such as shortness of breath, cough, and restrictive lung function patterns) are similar to those seen in common lung diseases, therefore the early diagnosis is a challenge. Some patients present for evaluation of cough and dyspnea several years before being diagnosed with ILD, after receiving initial diagnoses of chronic obstructive pulmonary disease, heart failure or other diseases.

Besides of the low prevalence, ILDs have no known clinical or radiological predictive biomarkers, only risk factors of low specificity associated with this disease have been identified (age, male sex, cigarette smoking, hepatitis C infection, history of tuberculosis, history of pneumonia, COPD, exposure to toxic substances [13]). Unless there is a specific suspicion for ILDs, the diagnosis can be easily overlooked. The incorrect or delayed diagnosis leads to worsening of the disease and the use of invasive and/or costly diagnostic procedures (like biopsies) of questionable value.

Accurate diagnosis and classification of ILDs often require input from various medical specialists, including pulmonologists, radiologists, pathologists, and rheumatologists. Coordinating and integrating the expertise of multiple disciplines is not easy, particularly in regions with limited access to specialized medical resources. Management of ILDs and care for patients with ILDs remain a challenge throughout the course of their disease for lack of disease-modifier treatment options.

2.2 Radiological challenges

The role of HRCT is critical for diagnosing ILDs. The different types of ILDs express specific imaging features like reticulation, consolidation, micronodules, emphysema, honeycombing, ground-glass opacity and a combination of these, that are essential for diagnosis. Interpreting radiological findings can be challenging as there is substantial inter-observer variability even between experienced radiologists, and the imaging patterns often are mixed, and the features observed overlap among different ILD subtypes. On the other hand, visual evaluation of ILD by HRCT has little sensitivity to objective changes in disease severity over short follow-up periods.

Image standardization is difficult to achieve, for normal lung tissue idiosyncrasy and artifacts, caused by patient movement during scanning, different types of breathing. Though HRCT is the accepted standard to be used when ILD is suspected, there are inconsistencies between CT technical characteristics, different scanner manufacturers, models, acquisition protocols, and reconstruction algorithms. International collaborations would be very important between Academia, Pharma Industry and Healthcare to develop comprehensive guidelines for imaging standards and basic image-processing algorithms.

The most clinically meaningful information hiding within the very large medical imaging datasets is generally unstructured, and require extensive preprocessing (including segmentation, filtering, registration, and labeling) before further analysis can occur. Defining the segment of interest for evaluation requires manual or semi-manual annotation.

2.3 Image processing challenges

Image standardization is difficult to achieve, for normal lung tissue idiosyncrasy, and artifacts caused by patient movement during scanning, different types of breathing. Though HRCT is the accepted standard to be used when ILD is suspected, there are inconsistencies between CT technical characteristics, different scanner manufacturers, models, acquisition protocols, and reconstruction algorithms. International collaborations would be very important between Academia, Pharmacological Industry and Healthcare to develop comprehensive guidelines for imaging standards and image-processing algorithms.

The most clinically meaningful information hiding within the very large medical imaging datasets is generally unstructured, and require extensive preprocessing (including filtering, registration, and labeling) before further analysis can occur. Defining the segment of interest for evaluation requires manual

or semi-manual annotation, therefore until the machine-learning mechanisms reach their advanced stage of development, human pre-processing remains essential.

The algorithms developed for image recognition still need to improve for the precise classification of the patterns seen (honeycombing, reticulation and ground glass opacity, etc.), especially when they appear mixed on the images studied. Multiple methods have been proposed for computer-aided object recognition and classifying (multi-scale rotation invariant algorithms with eg. Gabor filter, patch-based image representation methods and others), the optimal tool is yet to be found.

There is a pronounced need for a computer-based tool that operates on data from radiological images and clinical data, that predicts ILDs and/or reliably detects them at earlies (even subclinical) stages of the disease, and enables monitoring of disease response to therapy.

3 Digital techniques for ILD diagnosis and monitoring

There is a pronounced need for computer-based tools that operate on data from radiological images and clinical domain, that predict ILDs and/or reliably detect them at earlier (even subclinical) stages of the disease and enables their longitudinal follow up and assessing the treatment outcomes.

A few decades ago only simple image analytics were used for image processing purposes. The novel biomarkers based on radiography images have only started to become available recently, their numbers are steadily increasing with the implementation of complex image analysis based on machine learning techniques.

3.1 Quantitative CT

Quantitative CT (QCT) provides an alternative to the visual evaluation, that is objective and reproducible by the use of computer-based techniques to analyze HRCT images. This method is based on simple statistical analysis of CT attenuation values of each targeted pixel of the lung images, without studying the correlation between them [4].

The only method commercialized and widely used to-date to quantify the pulmonary tissue is CALIPER (Computer Aided Lung Informatics for Pathology Evaluation and Rating), developed by Mayo Clinic of USA. The im-

age quantification done by CALIPER is based on histogram signature mapping techniques trained through datasets confirmed by expert radiologists. As part of the development for ILDs, the local histograms computed from the $15 \times 15 \times 15$ neighborhood of each of the parenchymal voxel were compared against the histogram of exemplars identified in the training phase, divided in 5 classes (emphysema, ground glass opacity, honeycombing, reticular infiltrates and normal tissue). Quantitative discriminability of a number of pairwise dissimilarity metrics based on the volume of interest histograms was examined using multi-dimensional scaling. Of several techniques Cramer Von Mises Distance was found to be most consistent with the expert grouping. CALIPER is easy to use and provides good support for ILD diagnosis and disease course monitoring, its performance however leaves room for improvement. The correlation of CALIPER results with physiologic parameters was generally strong but the correlation with the radiologist assessment of disease type and severity was only around 50%, hence can only be used in the context of clinical data [7].

3.2 Complex networks

The new methods of computer aided diagnosis (CAD) for lung HRCTs only provide a static evaluation of the images and require extensive computing skills and infrastructure. In response to this challenge, a novel technique was developed by Truşculescu et al. [31], built on a CN analytic approach for imagistic aided diagnosis fitness for the possibility of achieving relevant data for ILD management.

The method was developed on HRCT images from 65 patients with ILD and 31 with normal lung, acquired from Clinical Hospital of Infectious Diseases and Pneumophysiology Dr. Victor Babeș of Timisoara, Romania. Regions of interest were marked by a radiologist with high experience in imagistic diagnosing of ILDs. Three non-overlapping separate bands of Hounsfield Units (HU) have been created in line with the categories of the characteristic attenuations of the lung alterations. The images were then transformed into complex networks according to specific predefined attachment rules, based on the HU values of each pixel. Network nodes and connections have been defined based on the similarities in HU values of neighboring pixels. CN measurements were done for interconnectedness and size. Maximum degree number, total degree count and average degree count were evaluated.

The method was successful for early disease detection in one of the three bands (the one corresponding to ground glass opacity), partially successful in

the other (reticulation) and not successful in the third (emphysema). When used to assess disease course on sequential image sets for the same patient, the method was highly successful by showing close correlation with the changes of the clinical parameters [31].

3.3 Convolutional neural network-based methods

Substantial progress has been made in image recognition, with the advent of CNN-based solutions following the availability of large-scale annotated datasets like ImageNet which offered very comprehensive database of more than 1.2 million categorized natural images of 1000+ classes [15]. Obtaining datasets as comprehensively annotated as ImageNet in the medical imaging domain remains a challenge however, as data acquisition is difficult, and quality annotation is costly.

The implementation of machine-learning-based image analysis in the clinical management of ILDs requires extensive data sets for training purposes. Given the rarity of ILD access to high-quality medical images and clinical data is costly and difficult.

Tables 1 and 2 summarize the results achieved by a selection of CNN-based methods deployed in ILD prediction and diagnosis, presenting details of the application, information on the used data volume, and the main performance benchmark values claimed by the authors.

The solutions developed for detecting ILD patterns are broadly divided into two categories: patch-based methods and slice-based methods, with the desire to trend towards the latter, which allows a more generalized processing of images, without the tedious manual work of the patch-based techniques.

3.3.1 Patch-based methods

A plethora of published works refer to patch-based classification of ILD patterns, after manual extraction of patches by radiologists [29]. Informative features are extracted from several ILD patches with the help of different feature extraction techniques for the classification of ILD patterns. The selection of an appropriate classifier is very important. Common methods used are k-nearest neighbors [24], artificial neural network, and support vector machines [19].

The classification accuracy of these methods steadily increased over time. An early method involving near-affine-invariant texture-based feature descriptor based on wavelet transformation used to classify the five ILD patterns (healthy, emphysema, GGO, fibrosis, and micronodules) showed a classifica-

Paper	Population	Data volume	Clinical application	Method	Results
Kim et al [21]	ILD	1200 ROIs	ILD features identification	Radiologist-identified ROIs, paired with a CNN classifier	$ACC = 81.27 - 95.12\%$
Christe et al 2019 [14]	IPF	105 cases	ILD features classification	CAD system using a CNN trained by radiologists	$F1 = 56\%$, $ACC = 81\%$
Agarwala et al [1]	ILD	1946 ROIs	ILD features identification	Radiologist-identified ROIs, paired with a CNN classifier, using faster R-CNN based detector network	$F1 = 55 - 88\%$
Huang et al [19]	ILD	unknown	ILD features classification	Unsupervised deep CNN	$F1 = 97.91\%$
Bermejo-Peláez et al [9]	ILD	37,424 ROIs	Automated identification and classification of ILDs	multi-model ensemble of deep CNN	Average $TPR = 91.41\%$, $TNR = 98.18\%$
Anthimopoulos et al [2]	ILD	14,696 ROIs	Lung pattern classification	Deep CNN	$F1 = 85.47\%$
Anthimopoulos et al [3]	ILD	172 scans	Semantic segmentation of ILD patterns	CNN, dilated convolution	$ACC = 81.8\%$

Table 1: Relevant studies in ILD diagnosis

Paper	Population	Data volume	Clinical application	Method	Results
Choi et al [12]	IPF	516 cases, 500 image montages each	Correlation with progressive pulmonary fibrosis	Diagnostic probability of UIP, with a deep CNN	hazard ratio 1.73 (CI95%: 1.40-2.14, $p < 10^{-4}$)
Budzykowski et al [10]	IPF	169 patients, 6 ROIs each	Association with genetic biomarkers (TOLLIP, MUC5B), survival	Extraction of radiomic features, paired with a CNN classifier	nine first-order texture features and one fractal feature were correlated with TOLLIP-1 mutations (AUC: 0.54 to 0.74); five Laws' filter features were correlated with TOLLIP-2 mutations (AUC: 0.53 to 0.70)
Park et al [23]	IPF	193 patients	Analysis of predictive factors for a decline in forced vital capacity (FVC)	Texture-based automated system used in-house software to quantify six ILD imaging features vs changes in FVC values	Reticular Opacity (RO) is sole independent predictor for FVC decline (p = 0.012; adjusted odds ratio, 1.047). ROC for RO was 0.641, optimal RO cutoff value was 22.05% (sensitivity, 50.0%; specificity, 81.4%; negative predictive value, 89.1%).

Table 2: Relevant studies in ILD prognostication

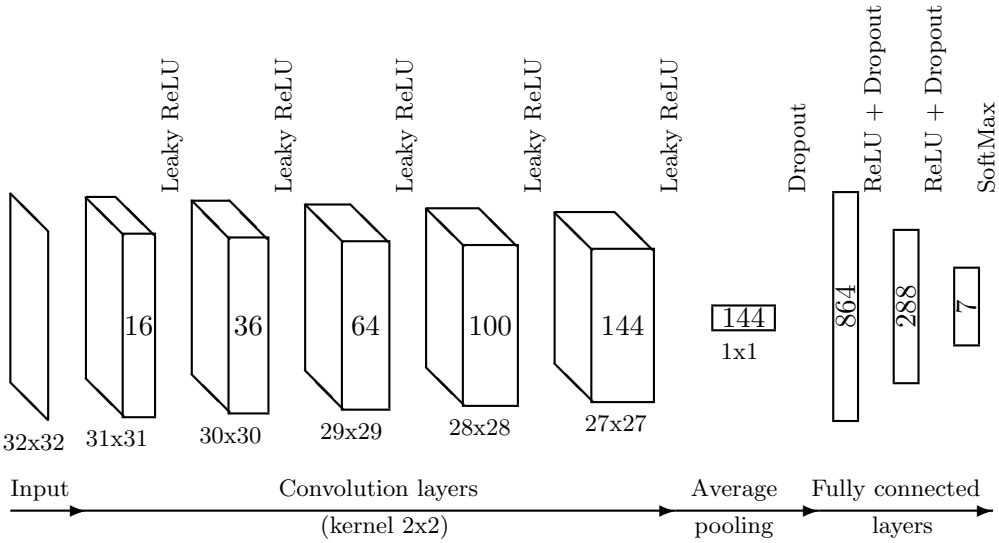

Figure 1: The structure of the CNN used for patch-based recognition of ILD, adapted from [2].

tion accuracy of 76.9% [16]. Another method based on texture and gradient features for patch-based classification of the ILD patterns using support vector machine, reported F1-scores ($F1 = 2 \times (\text{precision} \times \text{recall})/(\text{precision} + \text{recall})$) for healthy, emphysema, GGO, fibrosis, and micronodules are 84%, 75.3%, 78.2%, 84.1%, and 85.7%, respectively [28].

The first deep CNN designed for lung pattern classification achieved an average F1-score of 85.47% across 7 classes of CT image patches (6 typical ILD patterns and healthy tissue). The network, shown in Figure 1, was built of 5 convolutional layers, each of them used kernels of 2×2 and Leaky ReLU as activation function. The method used three dense layers with 7 outputs, in line with the ILD image classes targeted: ground glass opacity, micronodules, consolidation, reticulation, honeycombing and a combination of GGO/reticulation and healthy tissue. Training was done on a dataset of 14,696 image patches extracted from 120 HRCT images obtained from healthcare institutions [2].

More recently, another such method reported F1-score of 97.91%. This was achieved with a deep CNN architecture built from six different convolutional layers followed by batch normalization layers and ending with a fully connected layer. The network used input patches of size 32×32 extracted from ILD HRCT images. Each layer worked with kernel size of 2×2, with number of

kernels gradually increasing layer to layer from 32 to 192. ReLU was employed as activation function. The learning of unlabeled data was done through an unsupervised method. The results showed that the proposed CNN architecture outperforms most of the state-of-the-art ones [19].

Another promising method has been recently reported to identify radiographic patterns that precede the development of ILD with an average sensitivity of 91.41% and average specificity of 98.18% across 8 classes of HRCT pattern (healthy tissue, five interstitial features subtypes and two emphysematous classes), on 37,424 radiographic tissues extracted from 208 CT images. Deep learning approach was used on a highly complex ensemble of CNN architecture that comprises three different architectures such as 2D, 2.5D, and 3D for the classification of ILD abnormalities. Each individual network was trained from scratch from the database, the outputs of the networks are summed up in a weighted manner and combined to form the overall output of the ensemble. The resulting ensemble achieved a higher performance compared to each of the individual models, and the reported CNN methods of the domain, showing the potential of combined use of a suite of classifiers [9]. The network architectures involved in this study are depicted in Figure 2.

The results achieved with patch-based classification methods are remarkable, however their use is limited by computational challenges, the manual annotation involved and their limitation to be used for screening of HRCT patterns at slice level.

3.3.2 Slice-based methods

Early attempts to classify HRCT slices depending on the presence of pathology used pretrained AlexNet, but reported poor classification results. More complex solutions testing multiple systems (Cifarnet, AlexNet, GoogLeNet) showed improved slice level classification accuracy of ILD patterns on HRCT slices, the highest F1-Score achieved being with GoogLeNet, of 92% [27]. Details of the deployed network structures are given in Figure 3.

Deep CNN network with dilated filters were reported to be successful to segmentation of ILD patterns. The network proposed used input images of any arbitrary size of lung HRCT and the generated outputs were label maps. The network, as shown in Figure 4, consisted of eight convolutional layers having different dilation rates that increase exponentially. This helped to increase the receptive field while linearly growing the number of parameters. The performance was evaluated on 172 HRCT slices collected from two hospitals such

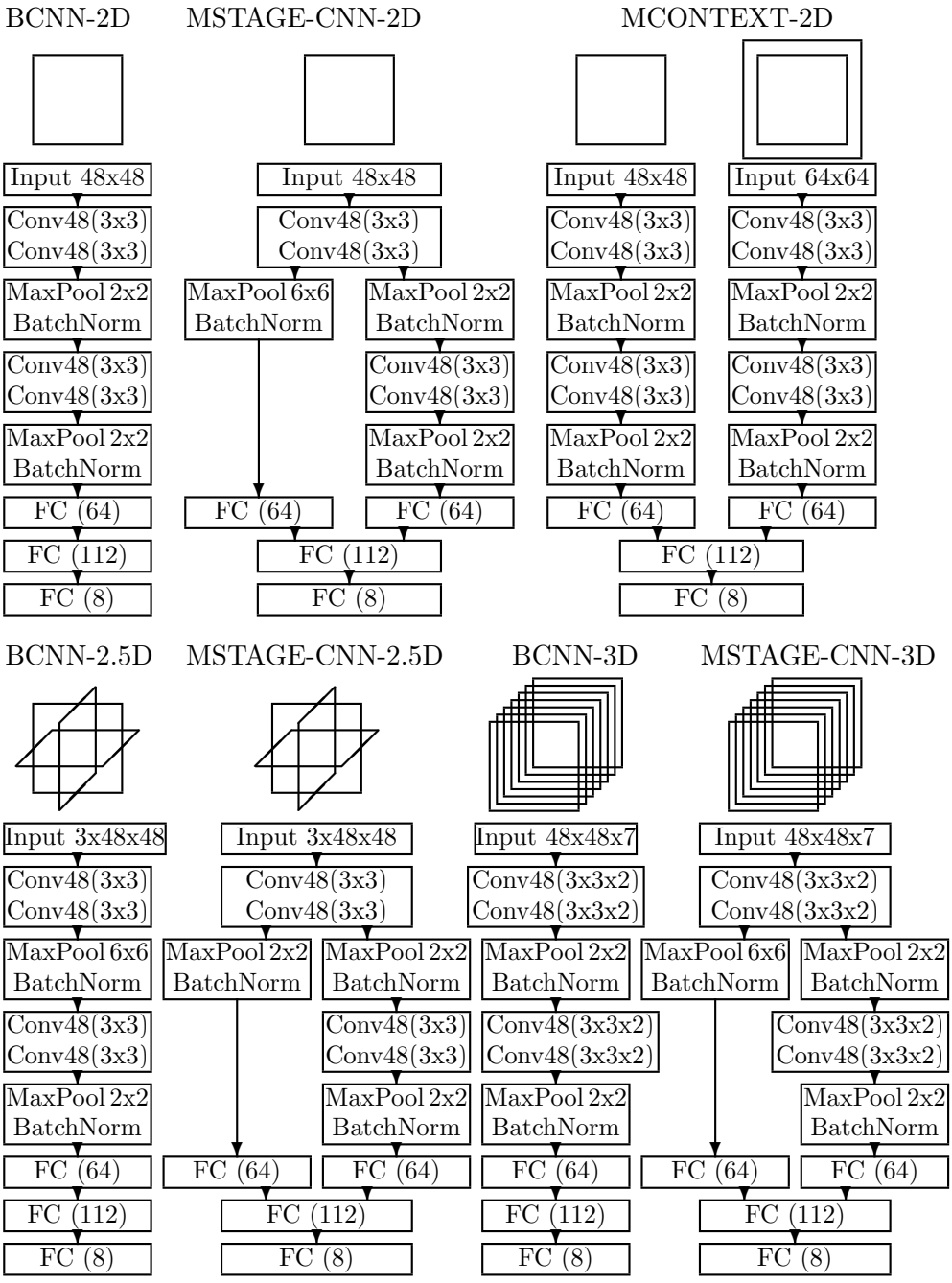

Figure 2: The CNN structures proposed by Bermejo-Peláez et al. [9].

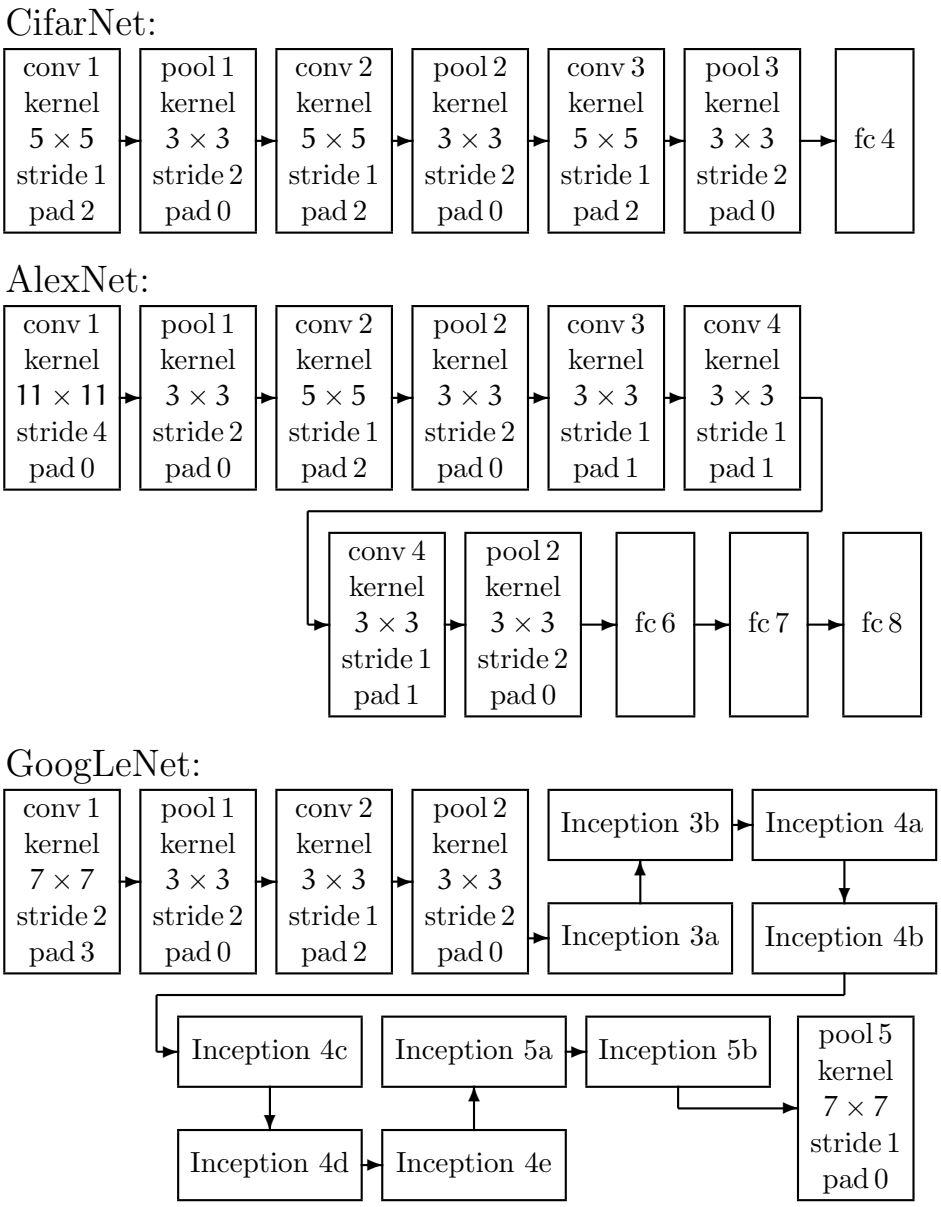

Figure 3: CNN architectures proposed by Shin et al, adapted from [27]. Each Inception module contains six convolution layers, a pooling layer and a concatenate layer.

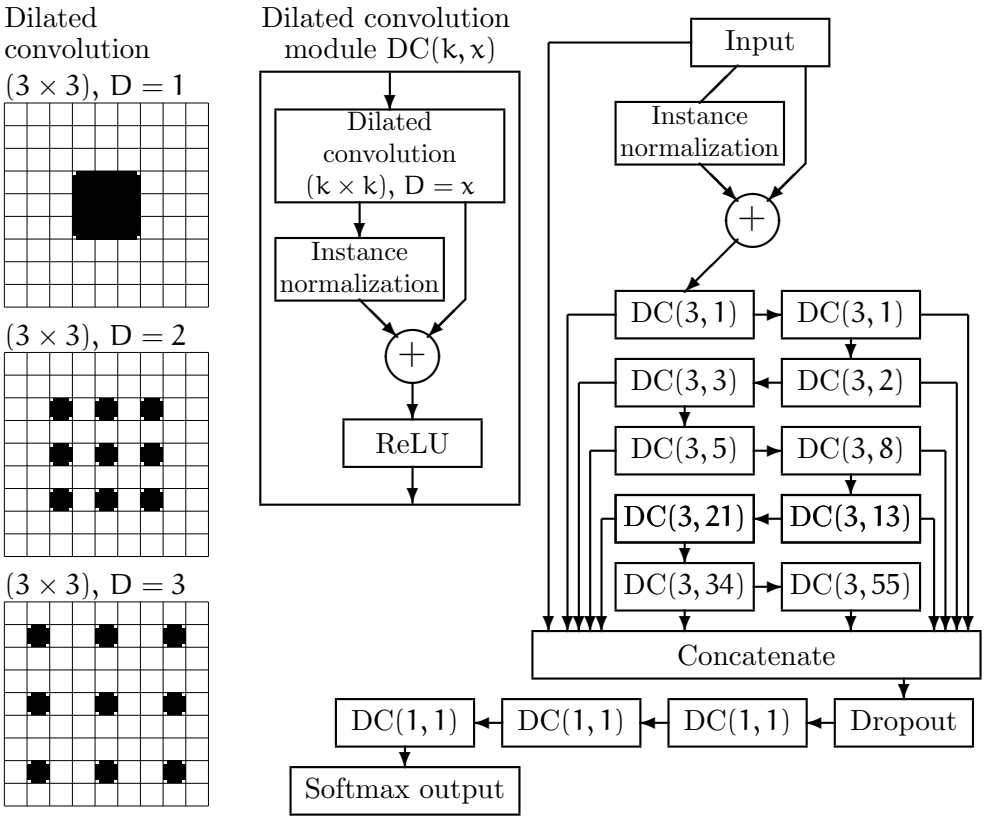

Figure 4: The CNN structure proposed by Anthimopoulos et al, adapted from [3]

as Geneva University Hospital and Bern University Hospital. This network achieved an accuracy of 81.8% [3].

Agarwala et al. [1] proposed a solution for localization of the typical ILD patterns in a HRCT slice using a more efficient region-based convolutional network (R-CNN) driven object detection network. GoogLeNet architecture has been modified for lower complexity by using only 5 inception blocks instead of 9 and used to extract the image features for faster object detection. The features provided by the fifth inception block were used as proposal for finding the targeted region. To overcome the limited amount of annotated training data, data augmentation techniques (flip, rotation, change of contrast, and addition of Gaussian noise) have been used. Six ILD patterns have been used (Consolidation, Emphysema, Fibrosis, GGO, Micronodule and healthy tissue).

The above-oultined method performed very well across all patterns, little less for fibrosis, achieving F1-scores between 0.55 and 0.86. It is fast and accurate, avoids the hassles of lung field segmentation and could be used in the screening of ILD using HRCT image slices.

4 Public datasets of ILD-related images

Beyond the private datasets of Healthcare institutions, there are multiple data sources and registries for ILD patients that provide access to radiography images (mostly HRCT) and clinical data points for research purposes. The most widely used open data sources are discussed below.

4.1 Lung Tissue Research Consortium database

The Lung Tissue Research Consortium database (LTRC-DB[1]) was a resource program of the National Heart, Lung, and Blood Institute that provides CT scans, as well as biospecimens to researchers of the domain. The LTRC was established in 2005 by the National Institutes of Health based on a coalition of 4 major clinical centers from the USA: Mayo Clinic Rochester, University of Michigan–Ann Arbor, University of Pittsburgh, and Temple University. During its active years between 2005 to 2019, the LTRC's main task was to collect, store, and make available imaging samples and clinical data from patients with various types of lung diseases. The LTRC sample and data set was sourced from more than 4,200 patients, with over 100 of cases with one of the several forms of ILDs.

4.2 Multimedia database of Interstitial Lung Diseases

The multimedia database for ILDs (MD-ILD[2]) was developed as part of the Talisman project at the University Hospital of Geneva and is made publicly available. This highly valuable database is specific to ILDs, and contains standard HRCT image series of 10-mm slice spacing. Annotations of pathological lung segments together with clinical parameters from patients with pathologically proven diagnoses of ILDs have been obtained from expert radiologists and treating clinicians. There are 128 ILD cases in the database with one of the 13 histological diagnoses of ILDs, 108 image series are available with

[1] https://ltrcpublic.com
[2] http://medgift.hevs.ch/wordpress/databases/ild-database/

1,946 delineated polygons of annotated lung parenchyma patterns, along a comprehensive dataset of 99 clinical parameters related to ILDs.

4.3 Inselspital Interstitial Lung Diseases database

The Inselspital ILD database (INSEL-DB) is a smaller but very well structured library, which has two main parts, based on the accompanying annotations. The first part consists of 60 HRCT image series of 9-mm slice spacing lung scans with annotated tissue from 2 radiologists (INSEL-DB-Seg), and the second consists of 105 HRCT lung scans provided by the ILD board of Bern University Hospital. The HRCT scans have been collected retrospectively, between October 2015 and June 2017. Demographic, clinical and laboratory data for each patient (e.g. sex, age, smoking history, duration of illness, lung function tests, results of blood tests) was also collected and made available to researchers.

4.4 AIFPR: Australian Idiopathic Pulmonary Fibrosis registry

A large regional library of patients data has been developed in Australia by University of Sydney[3]. AIPFR has been developed in Australia by University of Sydney3 with IPF cases recorded between February 2011 and December 2020. A total of 21 sites participated across Australia and New Zealand collecting impressively large datasets from over 2,700 patients enrolled in the program. Longitudinal follow-up data was also collected every 6 months when possible. The dataset collected includes clinical parameters (PFT), patient reported outcome (PRO) data, HRCT images and blood samples data. Data collection finished on 31 December 2021, the data continues to be available for research.

4.5 Open Source Imaging Consortium (OSIC) data repository

OSIC, an international group of leading experts, established OSIC Data Repository[4] on 22nd of May, 2019. This global, not-for-profit organization is a cooperative and open-source effort between academia, healthcare and industry to enable rapid advances in the detection and diagnosis of these conditions through digital imaging and machine learning.

[3]https://www.sydney.edu.au/medicine-health/our-research/research-centres/aildr.html
[4]https://www.osicild.org/

OSIC was created to drive collaboration between distant partners and to unite their capabilities. It was created to use artificial intelligence and other technological advances to build, and learn from, the largest and most diverse image and clinical database for fibrotic lung diseases. To-date OSCI has over 15,000 anonymized scans with accompanying clinical data, with over 106,000 anonymized data points from 1,843 patients with various forms of ILD. The enrollment of participants is ongoing.

5 Discussion

Over the recent years a myriad of computational techniques emerged in the support of radiographic image processing for ILDs. The example solutions discussed in the earlier sections outline encouraging trends, but the breakthrough has not yet been achieved. Many of the developed tools are highly performing, the competition for finding the optimal method is advanced and still ongoing. An ultimate breakthrough might not be possible however without addressing the key needs in image standardization, harmonization of definitions and classifications. This is not uncommon in the field of digital image-processing. For example, the automatic segmentation of brain tumors based on MRI data has been a widely researched topic for at least three decades. The development of segmentation methodology in the beginnings was similar to the current case of ILD: research groups were elaborating methods and techniques based on own data collections, usually captured by a low number of medical devices. Consequently their methods may have learned specific features of tumors together with parameters of the imaging equipment. Further on, the accuracy benchmark values were not objectively comparable with each other, because not even the testing data differed from team to team, but also the goals of the segmentation. Some were using single channel MRI volumes or only slices (cross sections), others lately turned to multi-spectral volumetric MRI data [17]. It is also necessary to mention, that this field grew together with the spectacular advances in the available computation speed and dynamic storage space, and the latest revolution of artificial intelligence brought by CNNs and deep learning. But the greatest factor in the development of brain tumor segmentation techniques represents the Brain Tumor Segmentation (BraTS) challenge [22, 5] organized yearly since 2012 by the Medical Image Computation and Computer-Assisted Interventions (MICCAI[5]) conference, which provided the common data, common goals and a common evaluation framework. BraTS

[5] https://www.miccai.org

thus provoked the explosion in the field that is directly responsible for thousands of methods and works elaborated in this field. The amount of training and testing data, and also the variability of data sources widened year by year, and new questions or secondary goals were defined (e.g. give an estimate of the time the patient lived after the MRI data were recorded). The initial training dataset contained only 30 records, and they were not even formatted to the same volume size. The experience accumulated year by year made the BraTS challenge an easily accessible research for all, and this led to the exponential growth of developed methods. The whole arsenal of artificial intelligence got involved in various solutions not only in the direct classification of pixels, superpixels or patches, but also in the preprocessing of the data and postprocessing of the classification outcome to optimize the accuracy of the final result [18].

The history of BraTS could be considered a guideline in the field of automatic processing of ILD-related image and medical data. An open challenge could bring considerable advancement in the development of segmentation methods. The most appropriate goal to set could be the automatic segmentation (localization and quantification) of fibrotic tissues from series of chest CT scans that come from the same patient during observation time, and eventually to give some prognosis of the illness using further available medical data. As it was already stated, the organization of this challenge would require establishing a collection of ILD patient records, image data collected from multiple institutions and various CT scanners, each record accompanied by the same set of medical parameters, and a ground truth established by competent human experts. Building up these foundations could help the scientific community in understanding the background of ILDs and could cause spectacular advances in the methodology of ILD treatment.

6 Conclusion

Research on imaging biomarkers in ILD is advancing rapidly. Machine learning stands at the core of this process, supported by on deep-learning-based image analysis. Several clinical challenges could be addressed by this technology like the prediction, early detection and precise categorisation of ILDs, along the improved monitoring of the disease's natural course and response to therapy. The results seen with Quantitative CT, Complex Networks, and Convolutional Neural Networks hold the promise of a brighter future.

The accuracy of recognizing ILD features in HRCT images already exceeds 90% in some of the methods, however, the most precise techniques are still experimental and need advanced computational resources and substantial manual work for training and annotations. In an ideal world the image recognition techniques should be integrated onto the everyday Radiology and Pulmonology practice to operate on entire CT slices, without any specific pre-work from the radiologists. There are still unmet needs both to increase sensitivity and specificity of the methods, as well as to achieve solutions that run seamlessly on regular healthcare IT infrastructure. The integration of rapidly evolving digital biomarkers with the physiological, proteomic, and genomic data for patients will offer the greatest patient benefit.

Acknowledgements

This study was supported in part by the Consolidator Researcher Program of Óbuda University.

References

[1] S. Agarwala, A. Kumar, A.K. Dhara, S.B. Thakur, A. Sadhu, D. Nandi, Special Convolutional Neural Network for Identification and and Positioning of Interstitial Lung Disease Patterns in Computed Tomography Images, *Pattern Recognition and Image Analysis* **31**, 4 (2021) 730-738. ⇒155, 161

[2] M. Anthimopoulos, S. Christodoulidis, L. Ebner, A. Christe, S. Mougiakakou Lung Pattern Classification for Interstitial Lung Diseases Using a Deep Convolutional Neural Network, *IEEE Transactions on Medical Imaging* **35**, 5 (2016) 1207-1216. ⇒155, 157

[3] M. Anthimopoulos, S. Christodoulidis, L. Ebner, T. Geiser, A. Christe, S. Mougiakakou, Semantic Segmentation of Pathological Lung Tissue with Dilated Fully Convolutional Networks, *IEEE Journal of Biomedical and Health Informatics* **23**, 2 (2018) 714-722. ⇒155, 161

[4] S.Y. Ash, R. Harmouche, D.L. Lopez Vallejo, J.A. Villalba, K. Ostridge, R. Gunville, C.E. Come, J.O. Onieva, J.C. Ross, G.M. Hunninghake, S.Y. El-Chemaly, T.J. Doyle, P. Nardelli, G.V. Sanchez-Ferrero, H.J. Goldberg, I.O. Rosas, R. San Jose Estepar, G.R. Washko, Densitometric and local histogram based analysis of computed tomography images in patients with idiopathic pulmonary fibrosis, *Respiratory Research* **18** (2017) 45. ⇒152

[5] S. Bakas, M. Reyes, A. Jakab, S. Bauer, M. Rempfler, A. Crimi, M. Prastawa, et al., Identifying the best machine learning algorithms for brain tumor segmentation, progression assessment, and overall survival prediction in the BRATS challenge, arXiv (2019) 1181.02629v2. ⇒164

[6] H. Barnes, S.M. Humphries, P.M. George, D. Assayag, I. Glaspole, J.A. Mackintosh, T.J. Corte, M. Glassberg, K.A. Johannson, L. Calandriello, F. Felder, A. Wells, S. Walsh, Digital Technology and the Future of Interstitial Lung Diseases, *Lancet Digit Health* **5** (2023) e41-50. ⇒149

[7] B.J. Bartholmai, S. Raghunath, R.A. Karwoski, T. Moua, S. Rajagopalan, F. Maldonado, P.A. Decker, R.A. Robb, Quantitative CT Imaging of Interstitial Lung Diseases, *Journal of Thoracic Imaging* **28**, 5 (2013) 298-307. ⇒153

[8] K. Berger, R.J. Kaner, Diagnosis and Pharmacologic Management of Fibrotic Interstitial Lung Disease, *Life (Basel)* **13**, 3 (2023) 599. ⇒149

[9] D. Bermejo-Peláez, S.Y. Ash, G.R. Washko, R. San José Estépar, M.J. Ledesma-Carbayo, Classifcation of Interstitial Lung Abnormality Patterns with an Ensemble of Deep Convolutional Neural Networks, *Scientific Reports* **10** (2020) 338. ⇒155, 158, 159

[10] J.D. Budzikowski, J.J. Foy, A.A. Rashid, J.H. Chung, I. Noth, S.G. Armato, Radiomics-based assessment of idiopathic pulmonary fibrosis is associated with genetic mutations and patient survival, *Journal of Medical Imaging* **8**, 5 (2021) 031903. ⇒156

[11] P. Camus, https://www.pneumotox.com, The drug-induced respiratory disease website, last accessed 15 June 2023. ⇒148

[12] B. Choi, S.Y. Ash, Deep Learning–based Classification of Fibrotic Lung Disease: Can Computer Vision See the Future?, *American Journal of Respiratory and Critical Care Medicine* **206**, 7 (2022) 812-814. ⇒156

[13] W.I. Choi, S. Dauti, H.J. Kim, S.H. Park, J.S. Park, C.W. Lee, Risk factors for interstitial lung disease: a 9-year Nationwide population-based study, *BMC Pulmonary Medicine* **18** (2018) 96. ⇒150

[14] A. Christe, A.A. Peters, D. Drakopoulos, J.T. Heverhagen, T. Geiser, T. Stathopoulou, S. Christodoulidis, M. Anthimopoulos, S. Mougiakakou, G. Stavroula, L. Ebner, Computer-Aided Diagnosis of Pulmonary Fibrosis Using Deep Learning and CT Images, *Investigative Radiology* **54**, 10 (2019) 627-632. ⇒155

[15] J. Deng, W. Dong, R. Socher, L.J. Li, K. Li, L. Fei-Fei, ImageNet: A large-scale hierarchical image database, *IEEE Conference on Computer Vision and Pattern Recognition (CVPR)* (2009) pp. 248-255. ⇒154

[16] A. Depeursinge, D. Van de Ville, A. Platon, A. Geissbuhler, P.A. Poletti, H. Müller, Near-affine-invariant texture learning for lung tissue analysis using isotropic wavelet frames, *IEEE Transactions on Information Technology in Biomedicine* **16**, 4 (2012) 665-675. ⇒157

[17] N. Gordillo, E. Montseny, P. Sobrevilla, State of the art survey on MRI brain tumor segmentation, *Magnetic Resonance Imaging* **31** (2013) 1426-1438. ⇒164

[18] Á. Győrfi, L. Szilágyi, L. Kovács, A fully automatic procedure for brain tumor segmentation from multi-spectral MRI records using ensemble learning and atlas-based data enhancement, *Applied Sciences* **11** (2021) 564. ⇒165

[19] S. Huang, F.F. Lee, R. Miao, Q. Si, C. Lu, Q. Chen, A deep convolutional neural network architecture for interstitial lung disease pattern classification, *Medical & Biological Engineering & Computing* **58** (2020) 725-737. ⇒154, 155, 158

[20] B. Kaul, V. Cottin, H.K. Collard, C. Valenzuela, Variability in Global Prevalence of Interstitial Lung Disease, *Frontiers in Medicine* **8** (2021) 751181. ⇒147

[21] G.B. Kim, K.H. Jung, Y. Lee, H.J. Kim, N. Kim, S. Jun, J.B. Seo, D.A. Lynch, Comparison of Shallow and Deep Learning Methods on Classifying the Regional Pattern of Diffuse Lung Disease, *Journal of Digital Imaging* **31** (2018) 415-424. ⇒155

[22] B.H. Menze, A. Jakab, S. Bauer, J. Kalpathy-Cramer, K. Farahani, J. Kirby, et al., The multimodal brain tumor image segmentation benchmark (BRATS), *IEEE Transactions on Medical Imaging* **34**, 10 (2015) 1993-2024. ⇒164

[23] H.J. Park, S.M. Lee, J.W. Song, S.M. Lee, S.Y. Oh, N. Kim, J.B. Seo, Texture-Based Automated Quantitative Assessment of Regional Patterns on Initial CT in Patients With Idiopathic Pulmonary Fibrosis: Relationship to Decline in Forced Vital Capacity, *American Journal of Roentgenology* **207**, 5 (2016) 976-983. ⇒156

[24] S.C. Park, J. Tan, X.W. Wang, D. Lederman, J.K. Leader, S.H. Kim, B. Zheng, Computer-aided detection of early interstitial lung diseases using low-dose CT images, *Physics in Medicine & Biology* **56** (2011) 1139-1153. ⇒154

[25] C.A. Powell, S. Modi, H. Iwala, S. Takahashi, E.F. Smit, S. Siena, D.Y. Chang, E. Macpherson, A. Qin, J. Singh, C. Taitt, N. Shire, D. Ross Camidge, Pooled analysis of drug-related interstitial lung disease and/or pneumonitis in nine trastuzumab deruxtecan monotherapy studies, *ESMO Open* **7**, 4 (2022) 100544. ⇒148

[26] G. Raghu, M. Remy-Jardin, J.L. Myers, L. Richeldi, C.J. Ryerson, D.J. Lederer, et al., Diagnosis of idiopathic pulmonary fibrosis an official ATS/ERS/JRS/ALAT clinical practice guideline, *American Journal of Respiratory and Critical Care Medicine* **198**, 5 (2018) e44-e68. ⇒147, 150

[27] H.C. Shin, H.R. Roth, M.C Gao, L. Lu, Z.T. Xu, I. Nogues, J.H. Yao, D. Mollura, R.M. Summers, Deep convolutional neural networks for computer-aided detection: CNN architectures, dataset characteristics and transfer learning, *IEEE Transactions on Medical Imaging* **35**, 5 (2016) 1285-1298. ⇒158, 160

[28] Y. Song, W.D. Cai, Y. Zhou, D.D. Feng, Feature-based image patch approximation for lung tissue classification, *IEEE Transactions on Medical Imaging* **32**, 4 (2013) 797-808. ⇒157

[29] C. Szegedy, W.Liu, Y.Q. Jia, P. Sermanet, S. Reed, D. Anguelov, D. Erhan, V. Vanhoucke, A. Rabinovich, Going deeper with convolutions, *IEEE Conference on Computer Vision and Pattern Recognition (CVPR)* (2015) pp. 1-9. ⇒154

[30] A.A. Trușculescu, D. Manolescu, E. Tudorache, C. Oancea, Deep learning in interstitial lung disease – how long until daily practise, *European Radiology* **30**, (2020) 6285-6292. ⇒150

[31] A.A. Trușculescu, D.L. Manolescu, L. Broască, V.M. Ancușa, H. Ciocârlie, C.C. Pescaru, E. Vaștag, C.I. Oancea, Enhancing Imagistic Interstitial Lung Disease Diagnosis by Using Complex Networks, *Medicina (Kaunas)* **58**, 9 (2022) 1288. ⇒153, 154

[32] A. Wallis, K. Spinks, The diagnosis and management of interstitial lung diseases, *BMJ* **2015** (2015) 350:h2072. ⇒149

Received: June 29, 2023 • Revised: July 20, 2023